

CORROSION BEHAVIOR OF MATERIALS IN RO WATER CONTAINING 250-350 PPM CHLORIDE¹

Anees U. Malik and Ismail Andijani

Saline Water Desalination Research Institute
Saline Water Conversion Corporation (SWCC)
P.O.Box 8328, Al-Jubail 31951, Saudi Arabia.
E-mail: rdc@swcc.gov.sa

ABSTRACT

Reverse Osmosis (RO) water constitutes about 22% of total desalinated water produced in the world. The rest of the desalinated water is almost entirely from thermal distillation, such as multistage flash (MSF) evaporation and multi-effect desalination (MED) techniques. The RO permeate is more corrosive than water produced by thermal distillation due to its high dissolved salts (TDS) level, particularly chlorides. As the RO water is transported through cementitious or polymer lined pipelines, steel components like pumps, valves and pipes are likely to corrode, if proper material selection is not made. Not much information is available regarding the corrosion behavior of RO water towards the metallic materials particularly steels which form the bulk of constructional materials.

A study has been conducted to investigate the corrosion behavior of some structural materials which include carbon steel 1018, electroless nickel plated carbon steel 1018 ENP, austenitic stainless steel AISI 304, and martensitic stainless steels AISI 410, AISI 420 and AISI 431 in RO water. These materials have been the main constructional materials used in metallic components of pipelines in Saudi Arabia. Studies have been carried out under dynamic conditions (impingement under flow), static conditions (crevice formers) and in presence of an inhibitor (phosphate) using a dynamic test loop. High chromium steels (> 15% Cr) appear to provide good resistance where as low chromium steels (< 15% Cr) exhibit generally poor resistance under the above mentioned test conditions.

¹ This paper was presented at International Desalination Association (IDA) World Congress Conference held at Singapore in 2005.

1. INTRODUCTION

The multistage flash (MSF) process, involving multistage distillation of seawater at low pressure, and reverse osmosis (RO) based on the separation of fresh water from seawater through a semi-permeable membrane under high pressure, are the two main industrial processes used for the desalination in the Middle East. The materials on the inlet side of the RO module are exposed to seawater feed with a total dissolved solids (TDS) in excess of 45,000 ppm, while those on outlet side are exposed to a product water stream with a TDS of about 500 ppm and a reject brine stream containing TDS around 60,000 ppm. This high TDS RO product water is much more corrosive than MSF product water which has a TDS of about 10 ppm. The chloride content in water plays a predominant role in imparting corrosivity. The desalinated water which is used as the potable water is transported through a net work of internally cement lined or polymer coated pipelines. The RO product water in pipelines, when comes into contact with pumps, valves or other metallic components, has the capability to corrode these components. A survey of the literature indicates that although numerous references are available on corrosion resistant materials related to MSF but only limited references are available on such materials related to RO product water [1-7]. Therefore, a study concerning with the corrosion behavior of SWRO product water containing high TDS with chloride content up to 350 ppm, is important for selecting the right material for pipeline transporting RO product water.

A wide variety of constructional materials have been used in the pumps, valves and other equipment in a recently built 450 Km long internally cement lined steel pipeline transporting RO product water. In this study, tests have been carried out on six typical materials which are mainly used in the construction of pipeline and water pumping equipment. The materials include : carbon steel 1018 (CS 1018), electroless nickel plated carbon steel containing 30 μm thick plating of Ni metal (1018 ENP), austenitic stainless steel AISI 304 SS and martensitic stainless steels, AISI 410 SS, AISI 420 SS and AISI 431 SS. The experimental studies include: (i) Corrosion resistance test under operating condition (ii) Corrosion resistance test under shutdown conditions and (iii) Effect of phosphate dosing.

2. EXPERIMENTAL PROCEDURES

CS 1018, 1018 ENP, martensitic chromium stainless steels namely AISI 410 SS, AISI 420 SS and AISI 431 SS and austenitic stainless steel AISI 304 were used during the experiment (Table 1).

Tests were carried out on 4 types of deaerated water, namely (a) LLW and (b) ULW representing lower and upper limits of dissolved solids in water, respectively and (c) and (d) containing Zn hexameta phosphate (ZHMP) in LLW and ULW, respectively, (Table 2).

Electrochemical polarization studies were carried out using a computer controlled EG&G model 273 EG&G Potentiostat. The experiments were carried out using corrosion cell (EG&G model K0047) with saturated calomel, graphite and epoxy mounted metal sample as reference, counter and working electrodes, respectively. The details of the experimental set up are given previously [8]. After stabilization of rest potential (E_{corr}), the scan was taken at the rate of 10 mV/min in the range of -250 mV to +200 mV vs. E_{corr} . From each curve, the rest potential, E_{corr} , the potential at which the current passed through a value of zero during the sweep and b_c , the Tafel slope of cathodic hydrogen part of the curve were recorded automatically.

Multiple Crevice Assemblies which were used in the present test had a 30mm OD and 20mm ID, thus producing a 5mm annular crevice site. The whole assembly was torqued to 10N/mm² force between crevice former assembly and the sample.

Jet Impingement Tests (JIT) were performed by using a Cortest Jet Impingement Test Apparatus (JITA). Using JITA, samples were tested simultaneously using 2 numbers of plenums. The samples were attached to plenums (Fig. 1). Each plenum chamber consists of 12 nozzle ports with 1mm diameter orifice, thus allowing 24 numbers of samples to be tested in each test. The plenums were constructed totally from titanium. During the test the plenums were submerged in test solution tank with a capacity of 100 liters. The test solution temperature was controlled by a heater-chiller unit provided with JITA. Table 3 shows conditions under which JIT were carried out.

A close circuit re-circulation Dynamic Test Loop (DTL) was used to carry out the tests as per ASTM G 31-72 (reapproved 1990) for weight loss under dynamic conditions. Flow diagram of DTL system is shown in Fig. 2. Five samples were fixed at a time in each coupon holder. The test velocity was varied by varying the test coupon holder diameter and flow rate of loop. The test loop had a facility to monitor inlet and outlet pressures, temperature and flow rate on continuous basis. Online data monitoring of the system was carried out. Coupons were fixed in the two holders for 14 and 28 days duration tests, respectively. The corrosion rate was calculated using standard formula [7]. Table 4 lists the parameters which were maintained during the operation of DTL.

3. RESULTS AND DISCUSSION

3.1 Testings under Operating Conditions

To generate data relevant to corrosion resistance under pipeline operating conditions, JIT was carried out. In the JIT, a flow induced localized corrosion would occur when metals and alloys are subjected to water jets of specified velocity. Velocity has a major role in inducing corrosion. During JIT, the corrosion process is accelerated by the removal of protective corrosion products layer on the metal surface by the action of shear stress and turbulence of fluid flow. This would result in direct exposure of base metal to environmental agent and accelerate the metal dissolution. Tests were carried out at two temperatures namely, 35°C and 50°C and at a velocity of 10 m/sec representing velocity of flow normally encountered at the immediate vicinity of pump outlets of transmission lines. The corrosion rates of alloys, CS 1018, ENP 108, 410 SS and 420 SS after 28 days tests were found higher than those tested for 14 days tests whereas alloys 304 SS and 431 SS were free from corrosion (Table. 5). Increase in temperature also increases the corrosion rates in case of CS 1018, ENP 1018, 410 and 420 SS.

Effect of water velocity was analyzed in terms of extent of corrosion by the measurement of depth of impingement attack (DI) as a function of radius of Impingement (RI). Depth of impingement was measured on tested sample using a calibrated microscope. The results indicate that only carbon steel was susceptible for impingement corrosion (Table 6), however, the extent of corrosion was not significant. Other materials were free from impingement corrosion. All materials did show

impingement mark by way of stains and except carbon steel none of the materials had any evidence of material loss due to erosion corrosion (depth of impingement attack = 0).

Under phosphate dosing condition, the corrosion rates of carbon steel due to impingement were lowered because of the inhibitive effect of phosphate.

3.2 Testings under Shutdown Conditions

The studies were carried out to determine the corrosion resistance of the materials under shut down condition when water is stagnant in the pipeline. Two methods were employed to investigate corrosion resistance under shut down condition namely, electrochemical polarization and crevice corrosion test using multiple crevice assembly.

Potentiodynamic cyclic polarization tests have been successfully used to determine the materials pitting susceptibility on the basis of pitting potential, E_{pit} . A noble value of pitting potential is taken to indicate a high resistance of material to pitting. Tests were carried out at 20°C and 45°C. Typical tafel plots are shown in Figs. 3 to 6. There are two important features of the tafel plots: on inhibition, corrosion current, I_{corr} was shifted to lower value and corrosion potential, E_{corr} was shifted to more noble value indicating the positive role played by the phosphate in inhibiting the corrosion reaction. Figures 7 to 9 show some typical cyclic polarization curves for steels in presence of ULW water with or without addition of phosphate. In general, E_{pit} shifts to more active potential with increase in chloride concentration (Table 7). Cyclic polarization curves for 1018 ENP do not exhibit a well defined E_{pit} in LLW or ULW but addition of phosphate provided inhibiting effect by showing improved pitting resistance (Fig. 7). The pitting susceptibility is generally observed for rest of the materials. The most resistant material was found to be 304 SS in all test media (Table 7). Out of the three martensitic chromium steels (namely, 410SS, 420SS and 431SS), 431 SS had shown highest resistance to pitting followed by 420SS and 410SS in water containing no phosphate. Apart from 1018 ENP, the inhibitive effect of phosphate appears to be negative, vis-à-vis E_{pit} in all the alloys except 420 SS in LLW and 431 SS in ULW.

Crevice exposure tests were carried out in stagnant solution to generate data on crevice corrosion susceptibility of materials. In crevice exposure tests, the susceptibility to crevice attack was determined in terms of maximum pit depth after exposure to crevices. Four types of water were used in the crevice test at 45 °C for 30 days : (i) ULW, (ii) LLW, (iii) ULW containing 2 ppm of phosphate and (iv) LLW containing 2 ppm phosphate. The procedures followed in the tests were as per ASTM G 78 - 89 for crevice testing.

No pitting was observed in alloys 304 SS and 1018 SS ENP and the alloys appeared to be free from crevice corrosion attack in LLW and ULW (Table 8). The carbon steel showed high corrosion rates in both LLW and ULW with LLW showing no crevice attack. It appeared that in high chloride medium, carbon steel underwent pitting and showed significant local attack. Alloy 420 SS showed maximum pit depth and highest number of pits. The presence of phosphate in general, had considerably reduced the overall corrosion rates and maximum depth of attack when compared to the tests without phosphate. Apart from CS 1018, alloys 304 SS, 431 SS and 1018 ENP were free from crevice attack in phosphate medium. The material 420 SS had the highest number of pits, however, depth of attack was lower when compared to test without phosphate addition (Table 8).

It appeared from the results of crevice corrosion studies that 304 SS was free from pits in all the four tests. The maximum depth of attack was experienced by 420SS followed by 410SS when compared to other alloys. Addition of phosphate resulted in pronounced inhibitive effect by total elimination of crevice attack in carbon steel 1018 and 431SS. Such inhibitive effect was not noticed in ENP-1018, but it showed inhibiting effect at low concentration of chloride (LLW with 2 ppm phosphate).

3.3 Effect of Phosphate Dosing (Dynamic Condition)

The effect of phosphate dosing on the corrosion behavior of alloys in high chloride water (ULW) under dynamic conditions was studied using a recirculation DTL as per ASTM G 31-72 (reapproved 1990). The test solution (ULW) was dozed sequentially with 0, 2 and 15 ppm ZHMP with a flow velocity of 4m/sec. The durations of the test were 14 and 28 days and the temperature was maintained at $40 \pm 3^{\circ}\text{C}$.

Exposure of CS 1018, 410 SS, 420 SS and 431 SS resulted in the growth of loose thick brown scales of iron oxides. The scales were easily removable. CS 1018 showed a uniform metal loss, 410 SS showed large number of pits over the edges whereas in 420 SS and 431 SS coupons no pitting was observed. Exposure of CS 1018 coupons exposed to ZHMP dozed ULW resulted in the formation of brownish grey adherent scales which appeared to be protective irrespective of duration of exposure.

The corrosion rate of carbon steel 1018 without ZHMP addition was highest followed by 410 SS and 1018 ENP, respectively. The alloys 420 SS and 431 SS showed negligible corrosion rates (Table 9). Addition of 2 ppm ZHMP decreased the corrosion rate of CS 1018 by one third and further addition up to 15 ppm ZHMP lowered down the corrosion rate by one fifth (Table 9 and Fig. 10). The maximum efficiency of the inhibitor was noted in the CS coupons. Addition of 2 ppm inhibitor showed an efficiency of 75% while on increasing the inhibitor concentration to 15 ppm, its efficiency increased to about 80% only. This showed that the effect of increasing the inhibitor concentration (from 2 to 15 ppm) on the efficiency of inhibitor was marginal. An increase in number of pits was observed when the inhibitor concentration was increased from 2 to 15 ppm. The number of pits in CS coupons also increased with increase in exposure period in presence of inhibitor.

4 CONCLUSIONS

- Under dynamic conditions, CS 1018 corroded significantly in RO water due to impingement. 304 SS and 431 SS do not corrode.
- Under dynamic conditions, the corrosion rate of CS 1018 are lowered down remarkably.
- Under shut down conditions, 304 SS is best resistant and CS 1018 is least resistant to RO water.
- Under shut down conditions, 304 SS is free from crevice effect in RO water.
- In general, the phosphate dosing annuls the effect of crevices in carbon steel, ferritic and austenitic steels in RO Water.

5 REFERENCES

1. J.W. Oldfield and B. Todd, Desalination, **55**, (1985), p. 261.
2. S. Nordin and J. Olsson, Desalination, **62**, (1987), p. 235.
3. A.M. Hassan, and A.U.Malik, Desalination, **74**, (1989), p. 157.
4. J.Nordström and J. Olsson, Desalination, **97**, (1994), p. 213.
5. J.W. Oldfield and B. Todd, Desalination, **108**, (1996), p. 27.
6. A. Al-Odwani, M. al-Tabtabaei and A. Abdul Nabi, Desalination, **120**, (1998), p.73.
7. M.G. Fontana, Corrosion Engineering (Singapore, McGraw-Hill International Edition 1987), p. 14.
8. A.U. Malik, N.A. Siddiqui, S. Ahmed and I.N. Andijani, Corrosion Sci., **33**, 1809, (1992).

Table 1. Chemical Composition of the Alloys used in Testing Program

S. #	Alloy	AISI Type	UNS No.	% C	% Cr	% Ni	Other Elements
1	Carbon Steel	CS 1018	J2503	0.25 max.	0.5 max.	0.5 max.	Cu 0.3 max. Si 0.6 max.
2	Electroless Nickel Plated Carbon Steel*	1018ENP	-	-	-	-	-
3	Austenitic Stainless steel	304SS	S30400	0.08 max.	18-20	8-12	-
4	Martensitic Chromium Stainless Steel	410SS	S41000	0.15 max.	11.5-13.5	-	-
5	Martensitic Chromium Stainless Steel	420SS	S42000	0.35-0.45 max.	12-14	0.5 max.	-
6	Martensitic Chromium Stainless Steel	431SS	S43100	0.2 max.	15-17	1.25-2.5	-

- 30 μm thick plating of Nickel metal on carbon steel

Table 2. Composition of RO Waters used in Testing Program

Concentration	LLW	ULW
Sodium (ppm)	160	225
Chloride (ppm)	250	350
Sulfate (ppm)	14	20
pH	8.5	8.5

Table 3. Test Conditions for Jet Impingement Tests

Test No.	Test Medium	Temperature °C	Velocity m/Sec	No. of Samples	Test period (days)
1	ULW	35 °C	10	2 sets of 12 each	14 and 28
2	ULW	50 °C	10	2 sets of 12 each	14 and 28
3	ULW+2 PPM ZHMP	35 °C	10	2 sets of 12 each	14 and 28

Table 4. Dynamic test loop operation

Test #	Mean Temperature (°C)	Inlet Pressure (bar)	Average Flow Rate (m ³ /hr)	Average Velocity (m/Sec)	ZHMP (ppm)
1	39.6	2.0	68.5	4.0	0
2	43.5	2.0	68.4	4.0	2
3	43.8	2.0	68.4	4.0	15

Table 5. JIT Results

Alloy	Test Sol.	Temp °C	CR mpy	Test Sol.	Temp °C	CR mpy	Test Sol.	Temp °C	CR mpy
1018	ULW	50 °C	29	ULW	35 °	28.0	ULW + 2% ZHMP	35 °C	6.0
1018 ENP	"	"	1.3	"	"	1.1	"	"	1.0
304 SS	"	"	0	"	"	0	"	"	0
410 SS	"	"	5.3	"	"	4.8	"	"	0.4
420 SS	"	"	1.7	"	"	1.1	"	"	0.1
431 SS	"	"	0	"	"	0	"	"	0

Table 6. Radius of Impingement (RI) and Depth of Impingement (DI) Data in RO Waters

Test Media Temp. Alloy	Parameter	ULW – 50 °C		ULW – 35 °C		ULW + 2 ppm Phosphate 35 °C	
		RI (mm)	DI(mm)	RI (mm)	DI (mm)	RI (mm)	DI (mm)
1018		35	0.31	30	0.6	15	0
1018 ENP		25	0	30	0	16.5	0
304		20	0	30	0	1	0
410		30	0	15	0	1	0
420		1	0	1	0	1	0
431		15	0	20	0	1	0

Table 7. Results obtained from cyclic polarization test under shut down conditions

Alloys	<u>LLW, 45°C</u>		<u>LLW, 45°C + ZHMP</u>		<u>ULW, 45°C</u>		<u>ULW, 45°C + ZHMP</u>	
	E_{Corr}	E_{Pit}	E_{Corr}	E_{Pit}	E_{Corr}	E_{Pit}	E_{Corr}	E_{Pit}
410 SS	-783	-12	-771	-60	-793	-36	-791	-36
420 SS	-802	185	-790	203	-799	60	-809	-61
431 SS	-748	390	-738	352	-762	263	-764	425
304 SS	-765	465	-753	433	-788	388	-780	344
1018 ENP	-485	-20	-448	153	-440	-22	-325	259

Test solution pH = 8.5, at 45°C in deaerated LLW and ULW with and without 2.0 ppm ZHMP

Table 8. Crevice test results at 45 °C

Alloy	Test solution	CR (mpy)	No. of Pits	Max. pit depth (mm)
1018	ULW	16.5	16	0.16
1018 ENP	"	3.1	0	-
304	"	0.0	0	-
410	"	2.1	21	1.2
420	"	1.25	26	1.4
431	"	0.0	1	0.3
1018	LLW	17.2	0	-
1018 ENP	"	2.3	0	-
304	"	0.0	0	-
410	"	19.5	27	0.45
420	"	0.35	37	1.4
431	"	1.0	1	0.6
1018	ULW + 2 ppm phosphate	5.0	-	-
1018 ENP	"	1.0	1	0.2
304	"	0.0	-	-
410	"	0.8	24	0.3
420	"	0.5	39	1.2
431	"	0.0	-	-
1018	LLW + 2 ppm phosphate	4.2	-	-
1018 ENP	"	0.5	-	-
304	"	0.0	-	-
410	"	0.5	15	0.1
420	"	0.8	35	1.2
431	"	0.0	-	-

Table 9. Corrosion rate and efficiency of phosphate inhibitor (ZHMP) from dynamic test loop

ZHMP	Materials							
	<u>Carbon Steel</u>		<u>1018 ENP</u>		<u>410 SS</u>		<u>420 SS</u>	<u>431 SS</u>
	CR mpy	% efficiency	CR mpy	% efficiency	CR mpy	% efficiency	CR mpy	% efficiency
0	114.1	0	2.3	0	3.4	0	0	0
2	37.9	66.8	1.7	26.0	2.6	23.6	0	100
15	22.2	80.6	0.8	65.2	2.6	25.1	0	100

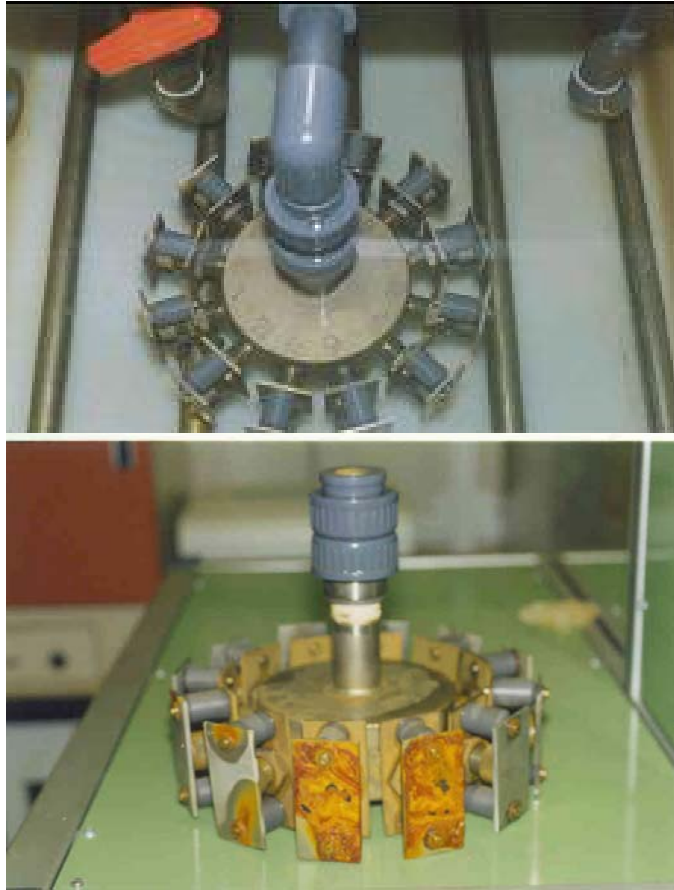
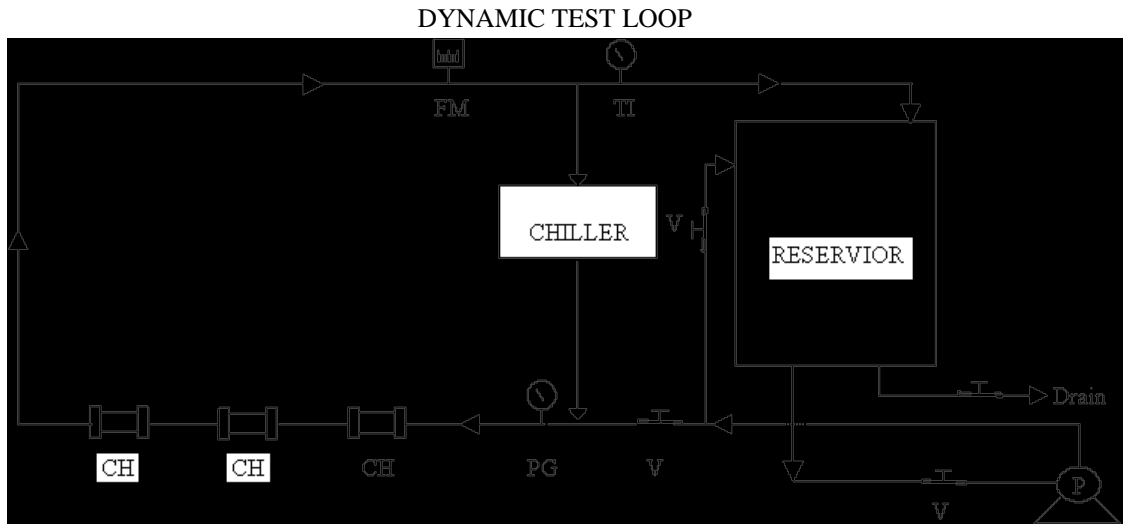


Figure 1. Photographs of plenum used for testing of samples in JITA



- | | | | | | |
|----|---|----------------|----|---|-----------------------|
| CH | = | Coupon Holder | PG | = | Pressure Gauge |
| FM | = | Flow Meter | TI | = | Temperature Indicator |
| OM | = | Oxygen Monitor | V | = | Valve |
| P | = | Pump | | | |

Figure 2. Flow Diagram of Dynamic Test Loop

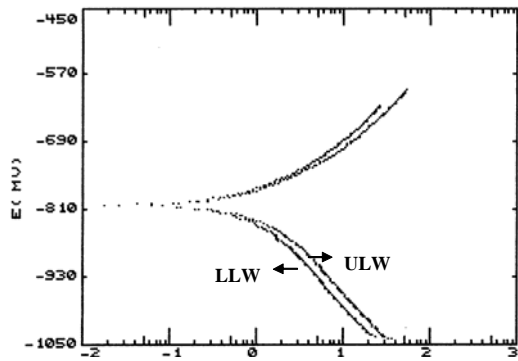


Figure 3. Tafel plots of carbon steel in two different test solutions at 20°C

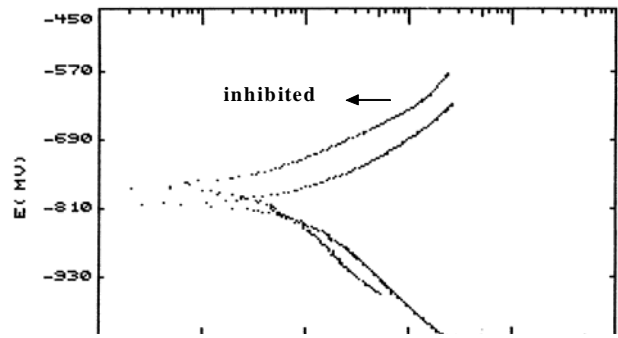


Figure 4. Tafel plots of carbon steel in LLW solution at 20°C with and without corrosion inhibitor

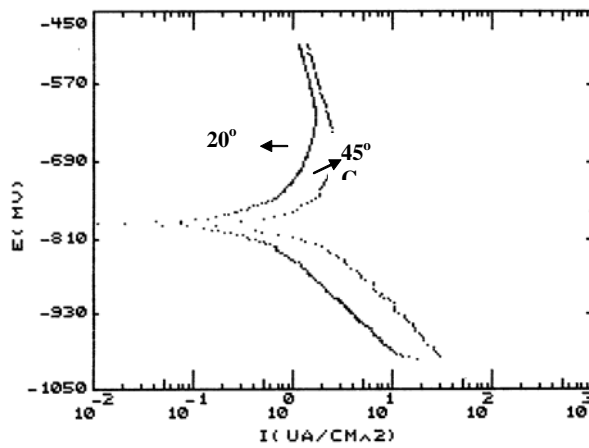


Figure 5. Tafel plots of SS 410 in LLW solution at 20 and 45°C

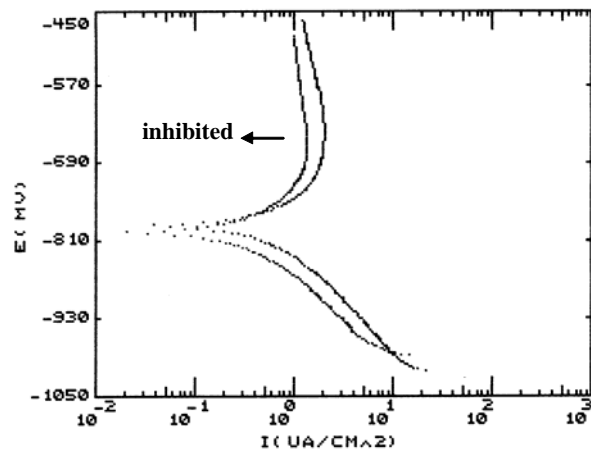


Figure 6. Tafel plots of SS 420 in LLW solution at 20°C with and without phosphate (corrosion inhibitor)

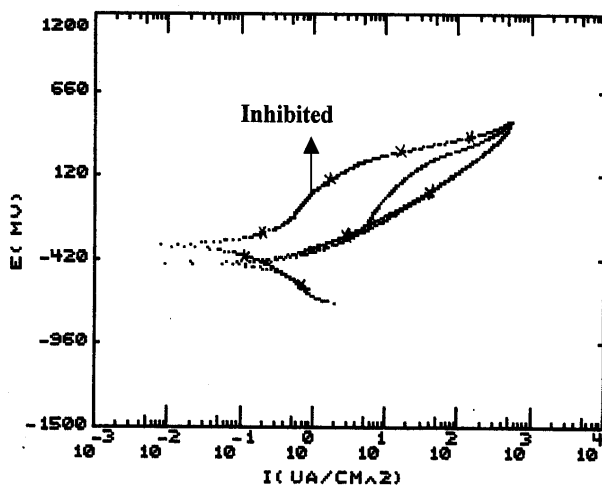


Figure 7. Cyclic polarization curves of 1018-ENP in deaerated ULW solutions with and without inhibitor at 45°C

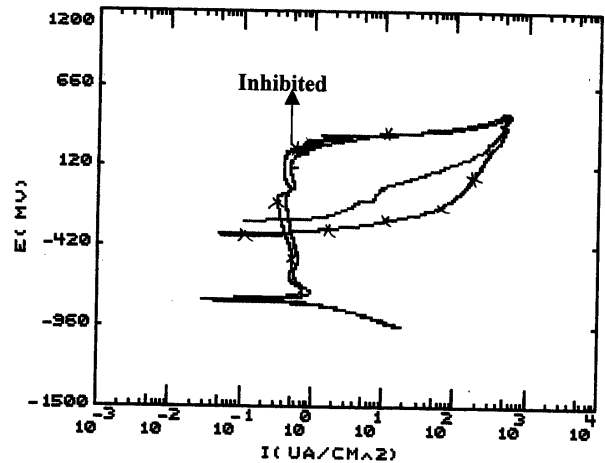


Figure 8. Cyclic polarization curves of 304 ss in deaerated ULW solutions with and without inhibitor at 45°C

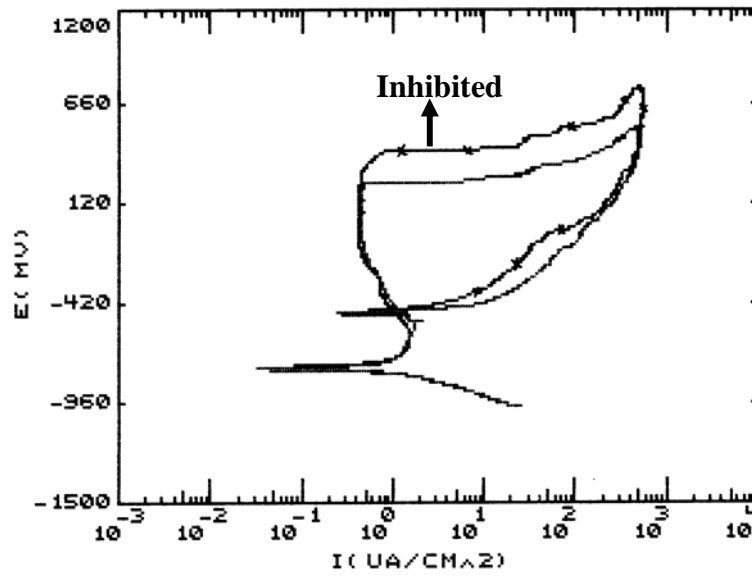


Figure 9. Cyclic polarization curves of SS431 in deaerated ULW solution with and without inhibitor at 45°C

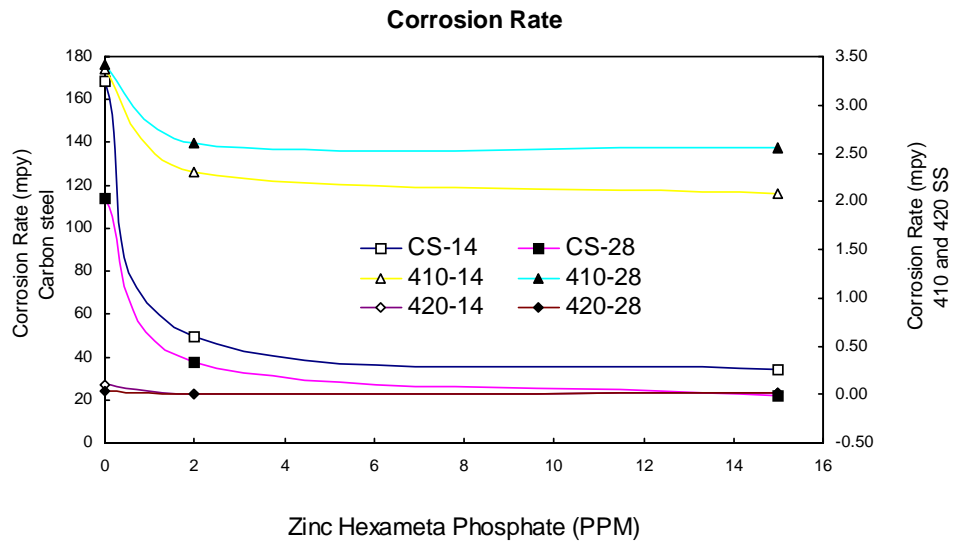


Figure 10. Graphs Showing the Variation of Corrosion Rates of CS-1018, 410 SS and 420 SS after 14 and 28 days exposures